

## CHARACTERIZATION OF A SUB-MM WAVE FREQUENCY SELECTIVE SURFACE ON A PERIODICALLY PERFORATED SILICON SUBSTRATE

Angel Colin\*

Instituto Nacional de Astrofísica, Óptica y Electrónica (INAOE), Luis Enrique Erro, No. 1, Santa María Tonanzintla, Puebla 72840, México

**Abstract**—We carried out measurements of optical transmission through a Frequency Selective Surface (FSS) on a silicon substrate perforated periodically with square cavities of  $1 \text{ mm}^2$ . The substrate is covered on one side with a thin film ( $1 \mu\text{m}$  thick) of silicon-nitride, thus forming a membrane for each cavity. The measurements were taken using a Martin-Puplett Interferometer over a spectral range from 100 to 650 GHz, providing a maximum transmission value of around 40% at 480 GHz. Analytical and computed results are also presented for comparison purposes.

### 1. INTRODUCTION

All thermal detectors used for astronomical observations in the ranges of mm and sub-millimeter waves, require to be characterized before being installed into a telescope. That implies the correct choice of additional elements to reduce their noise equivalent power and the use of filters to define their wave range of operation. Generally, there are three types of two-dimensional filters for these purposes: 1) a capacitive grid, composed by an arrangement of thin metallic geometries deposited periodically on a dielectric substrate, thus acting as low-pass filter. 2) An inductive mesh, the complement of the previous one, which acts as high-pass filter and can be composed by a wire screen. And 3) a resonant grid, composed by a periodic array of cross shaped holes which acts as a band-pass filter. These kinds of filters commonly called as Frequency Selective Surfaces (FSS), have been well described before in the literature [1, 2]. The FSS on

---

*Received 12 September 2012, Accepted 12 November 2012, Scheduled 14 November 2012*

\* Corresponding author: Angel Colin (angel.colin@inaoep.mx).

periodically perforated substrates are also used to support large focal plane arrays of bolometers, some examples can be seen in [3, 4], where such bolometers were built and deposited on silicon-nitride membranes suspended on micro-machined cavities into a silicon substrate.

In this paper we report measurements of optical transmission through a FSS on a high resistivity silicon substrate perforated periodically with square cavities of  $1 \text{ mm}^2$ , and covered on one side with a thin film ( $1 \mu\text{m}$  thick) of silicon-nitride, thus forming a membrane for each cavity. Analytical and computed results were experimentally verified by Fourier transform spectrometry using a Martin-Puplett Interferometer over a spectral range from 100 to 650 GHz. The spectral performance of this FSS presents a maximum transmission value around 40% at 480 GHz. The modeling was made using the commercial computer software (HFSS) based on the finite elements method. This kind of FSS has the advantage that can be used for several purposes for instance, as a band-pass filter as well as support for thermal detectors.

## 2. TRANSMISSION ANALYSIS

The theoretical analysis for the optical transmission through a periodically perforated substrate was made as follows.

Referring to Figure 1(b), the signal  $I$  transmitted through the substrate results from two contributions: a) the interference signal, and b) the Fabry-Pérot effect.

The interference is produced due to the phase difference between the signals passing through the silicon substrate and the cavities respectively. Therefore

$$I = (S_t - S_p) (1 - R) I_0 + S_p I_0 + 2 [(S_t - S_p) (1 - R) S_p]^{1/2} \cos \varphi I_0 \quad (1)$$

where  $S_t = 1256 \text{ mm}^2$ , is the optical surface analyzed in the substrate, corresponding to a circular area of 40 mm of diameter,  $S_p = 204 \text{ mm}^2$  is the total surface of the cavities, corresponding to the array presented in Figure 1(a), i.e., 204 square cavities of  $1 \text{ mm}^2$  each one,  $R = \left(\frac{n-1}{n+1}\right)^2 = 0.3$ , is the reflection coefficient of the silicon substrate with its optical index  $n = 3.45$ , and a phase delay  $\varphi = 2\pi f \frac{(n-1)t}{c}$ , where  $t = 270 \mu\text{m}$  is the thickness of the substrate, and  $f$  is the operation frequency in GHz.

b) The Fabry-Perót effect is due to the interference between a transmitted beam and the multiple reflections inside the substrate, therefore

$$I_{F-P} = \frac{S_t - S_p}{S_t} \frac{1}{1 + F \sin^2 \left( \frac{2\pi f}{c} n e \right)} \quad (2)$$

with  $F = \frac{4R}{(1-R)^2}$ .

According to design and technical characteristics of the Martin-Puplett interferometer, we have

$$\frac{I}{I_0} = 940 + 775 \cos(0.0138f) \tag{3}$$

$$I_{F-P} = \frac{0.8}{[1 + 2.5\sin^2(0.02f)]} \tag{4}$$

with  $f$  in GHz. The results of this analysis are plotted in Figure 4, where the analytical spectrum was estimated by the product of Equations (1) and (2).

### 3. TRANSMISSION MODELING WITH HFSS

The transmission modeling was performed using a commercial finite-element tool package (HFSS). The geometry was simulated for a single cavity with periodic boundary conditions, known as “master/slaves” in HFSS to truncate the infinite space to a finite volume. This

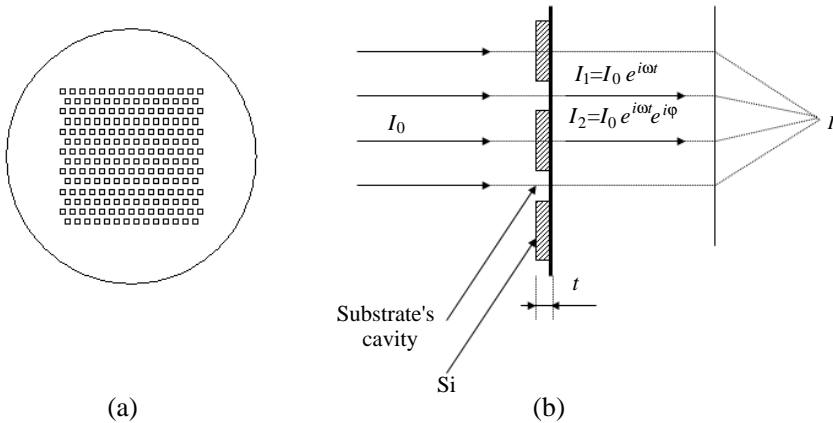


**Figure 1.** (a) Schematic arrangement (not to scale) of 204 square cavities of  $1\text{ mm}^2$  on a circular substrate of 50.8 mm of diameter. (b) Section detail of the substrate (not to scale) with membranes suspended on the cavities. The beam ( $I_0$ ) passing through substrate produces a signal delay ( $I_2$ ), which interfere with ( $I_1$ ). After that, both ( $I_1$ ) and ( $I_2$ ) are collimated thus forming the whole transmitted signal ( $I$ ).

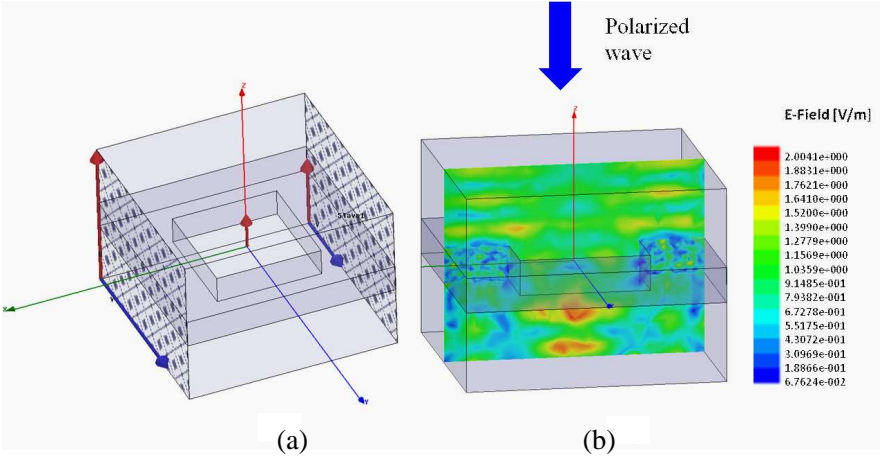


**Figure 2.** Modeling with HFSS. (a) Using periodic boundary conditions (master/slaves) extended to an infinite number of cavities at each side. (b) Animation with an incident polarized wave in a single cavity.

permits the analysis of thick substrates perforated periodically with arbitrary geometries, reducing the structure to a single unit cell defined by electric and magnetic walls. The periodicity is applied by the algorithms to the adjacent walls of the structure thus forming an array of  $n \times n$  elements as is shown in Figure 2(a). For our purposes, we extended the simulation in a frequency range from 100 GHz to 650 GHz over a unit cell with surface of  $4 \text{ mm}^2$  and a cavity of  $1 \text{ mm}^2$  using the following parameters: a) substrate material: Silicon, b) thickness  $t = 270 \text{ }\mu\text{m}$ , c) membrane only on one side:  $1 \text{ }\mu\text{m}$  thick of silicon-nitride, d) relative permittivity  $\varepsilon = 11.9$ , e) loss tangent  $LT = 0.04$ , f) conductivity  $\sigma = 10 \text{ Siemens/m}$ , g) refraction index  $n = 3.5$ , h) reflection coefficient  $R = 0.3$ , i) total surface  $S_t = 4 \text{ mm}^2$ , and j) surface of cavity  $S_p = 1 \text{ mm}^2$ .

An incident electromagnetic wave elliptically polarized and perpendicular to the surface was used to excite the structure. Hence, the electric and magnetic fields were calculated throughout the simulation volume. This allowed for the viewing and analysis of fields strengths and directions at critical locations in the simulation space, particularly in the air gap of the cavity as is shown in Figure 2(b). Here, one can appreciate the concentration of the electric field into the cavity, whereas the electric field strength turns to be symmetrically diminished into the substrate. That may be due to the material properties and

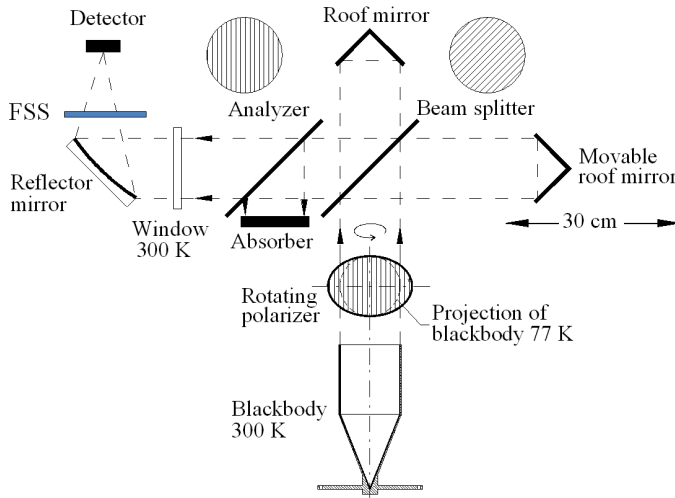


**Figure 3.** Schematic arrangement (not to scale) for measuring optical transmission with a Martin-Puplett interferometer.

thickness of the substrate which in turn produce a signal delay, as expected. The results of this performance are shown in Figure 4.

#### 4. TRANSMISSION MEASUREMENTS

The FSS was fabricated using a commercial silicon wafer of two inches (50.8 mm) of diameter with a chosen thickness of  $270\ \mu\text{m}$  to satisfy the Fabry-Pérot resonance condition [5]. The periodic micro-machining perforations and silicon-nitride deposition were realized with accurate standard microelectronics techniques.

The schematic setup for measuring the response of the FSS is shown in Figure 3, where the operational principle of the Martin-Puplett interferometer is based on two combined beams from two unpolarized radiation sources (blackbodies operating at 77 and 300 K, respectively). The beams are transmitted through the rotating polarizer, then divided in two partial beams by the beam splitter and flipped by the roof mirrors; hence the beam first transmitted at the beam splitter is now reflected and vice versa. The recombination of the beam will be elliptically polarized, depending on their path difference. After passing through the analyzer, one of the orthogonal components will be absorbed, whereas the second one will be transmitted and focused into the detector by a reflector mirror. The detector is a commercial 4.2 K bolometer in a Dewar, whose optics matches to the

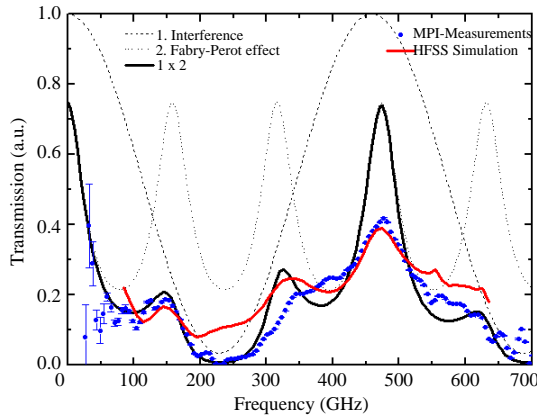


**Figure 4.** Transmission spectra. Blue dots with error bars correspond to measurements, the dark line is the product of two contributions from the analytical model, and the red line corresponds to simulation results with HFSS.

Martin-Puplett interferometer.

Three measurements were carried out to characterize the spectral response of the FSS following the methodology in [6]. In all cases, the FSS is at ambient temperature. The first measurement was realized by taking a data series of reference spectra with the FSS out of the beam, the second one, by taking a data series of reference spectra with the FSS in the beam, and the third one, with the FSS out of the beam. Both the first and the third measurements are averaged, then we divided the FSS spectrum by the average of the reference spectra. The result is the absolute spectral response. These last results with the previous analytical and computed spectra are depicted in Figure 4 for comparison purposes.

In Figure 4 we can appreciate that simulation results obtained with HFSS do not match the measurements as well as we expected. It should be taken into account that our model does not include the mechanical constraints for mounting and demounting the FSS, nor the optical losses caused by the physical setup with the Martin-Puplett interferometer and the Dewar, however the stop-band frequency from 200 to 300 GHz and the maximum transmission value of around 40% at 480 GHz follow similar behavior as the measured and the analytical spectra, providing a good agreement.

## 5. CONCLUSION

In this paper we have presented the experimental verification of a FSS on a periodically perforated silicon substrate acting as pass-band filter. Around 40% of absolute optical transmission is achieved at 480 GHz using a square configuration of 204 cavities of  $1 \text{ mm}^2$ . This kind of FSS can also be used to support large focal plane array of thermal detectors.

## REFERENCES

1. Ulrich, R., "Far-infrared properties of metallic mesh and its complementary structure," *Infrared Phys.*, Vol. 29, 37–55, 1967.
2. Porterfield, D. W., J. L. Hesler, R. Densing, E. R. Mueller, T. W. Crowe, and R. M. Weike, "Resonant metal-mesh bandpass filters for the far infrared," *Appl. Opt.*, Vol. 33, 6046–6052, 1994.
3. Siringo, G., et al., "The large APEX bolometer camera LABOCA," *Astron. & Astrophys.*, Vol. 497, 945–962, 2009.
4. Bidaud, A., et al., "Antenna-coupled arrays of NbSi microbolometers," *Exp. Astron.*, Vol. 32, 179–191, 2011.
5. Iodice, M., G. Cocorullo, F. G. Della Corte, and I. Rendina, "Silicon Fabry-Pérot filter for WDM systems channels monitoring," *Opt. Comm.*, Vol. 183, 415–418, 2000.
6. Page, L. A., E. S. Cheng, B. Golubovic, J. Gundersen, and S. S. Meyer, "Millimeter-submillimeter wavelength filter system," *Appl. Opt.*, Vol. 33, 11–23, 1994.